

Enhanced dielectric properties of Zn and Mn co-doped $\text{CaCu}_3\text{Ti}_4\text{O}_{12}$ ceramics

Zunping Xu¹ · Hua Qiang²

Received: 28 June 2016 / Accepted: 9 August 2016 / Published online: 11 August 2016
© Springer Science+Business Media New York 2016

Abstract Zn-doped and (Zn+Mn) co-doped $\text{CaCu}_3\text{Ti}_4\text{O}_{12}$ ceramics were prepared by the citrate–nitrate combustion derived powders in order to investigate the effect of dopants on the microstructure and electrical properties. The results showed that giant dielectric response was enhanced by co-doping of Zn and Mn. Compared with other samples, (Zn+Mn) co-doped ceramics exhibit a fine-grained microstructure. Much stronger nonohmic properties were realized in these ceramics. It is significant that the (Zn+Mn) co-doping effectively reduced the dielectric loss in the medium frequency region and at room temperature. At $x = 0.05$ and $y = 0.03$, low dielectric loss ~ 0.026 and moderate dielectric constant ~ 6620 were observed at room temperature and 10 kHz. The present results indicate that (Zn+Mn) co-doping may improve the dielectric properties and increase the grain boundary resistance of $\text{CaCu}_3\text{Ti}_4\text{O}_{12}$.

1 Introduction

There has been a considerable interest in the study of calcium copper titanate ($\text{CaCu}_3\text{Ti}_4\text{O}_{12}$, CCTO) due to its unusual giant dielectric constant (ϵ_r) of about 10^4 , good thermal stability in a wide temperature range from 100 to 600 K and high nonlinear coefficient (α) [1, 2]. In spite of the enhanced properties, the nature and origin of the giant

ϵ_r of CCTO remain controversial. Some studies showed that the microstructure and electrical properties of CCTO depend on processing routes [3–5]. Many methods were applied to enhance the dielectric properties of CCTO. Recently, much work based on partial substitution of Cu or Ti ions in CCTO ceramics has been carried out in order to improve the dielectric properties and to understand the origin of giant dielectric response in CCTO ceramics [6–9]. Partial isovalent ion substitution of Zr, Zn and Y in CCTO ceramics enhanced the dielectric response due to the modification of mixed-valent structure [10–12]. Xu et al. [6] reported that Zn-doped $\text{CaCu}_3\text{Ti}_4\text{O}_{12}$ ceramics have high ϵ_r and low dielectric loss ($\tan \delta$). Li et al. [13] reported that Mn doping significantly enhanced the grain boundary resistance of CCTO. Mn doping reduced both ϵ_r and $\tan \delta$ of CCTO [14] and BST [15]. By reducing the grain size to increase the density of grain boundaries layers, and then enhance the resistance of internal interfaces, so that reduce the $\tan \delta$ of CCTO-based compounds [16].

In this work, Zn-doped and (Zn+Mn) co-doped CCTO ceramics were fabricated by employing the powders obtained by the citrate precursor processing. The effect of different dopants on the microstructure and dielectric properties were analyzed and discussed.

2 Experimental

Undoped, Zn-doped and (Zn+Mn) co-doped CCTO ceramics with the nominal composition of $\text{CaCu}_{3-x}\text{Zn}_x\text{Ti}_{4-y/2}\text{Mn}_y\text{O}_{12}$ [$(x = 0.05$ and $y = 0, x = 0.05$ and $y = 0.03, \text{ and } x = 0.05$ and $y = 0.05)$], abbreviated as, CCTOM0, CCTOM3, and CCTOM5] were prepared by the citrate–nitrate combustion derived powders. Copper nitrate, calcium nitrate, tetrabutyl titanate and additions (zinc oxide

✉ Hua Qiang
qh20049@163.com

¹ Faculty of Materials and Energy, Southwest University, Chongqing 400715, China

² Chongqing College of Humanities, Science and Technology, Chongqing 401524, China

and manganese acetate) were used as the starting materials. The details of powders preparation process were described elsewhere [17]. The powders were calcined at 800 °C for 3 h in air and then uniaxially pressed into discs. Finally, the discs were sintered into ceramics at 1060 °C for 8 h in air.

The crystal structures of the sintered ceramics were confirmed by X-ray diffraction (XRD). The microstructure of the specimens was observed by scanning electron microscopy (SEM). The dielectric properties of the samples were measured using impedance analyzer (Agilent 4294A). The dielectric properties as a function of temperature were measured using precision LCR meter (E4980A). The voltage-current (V – I) characteristics were measured using a high voltage measurement unit (Model 247).

3 Results and discussion

Figure 1 shows the XRD patterns of sintered CCTO, CCTOM0, CCTOM3 and CCTOM5 ceramics. As shown in Fig. 1a, the cubic perovskite CCTO phase as the only phase and no secondary phases can be detected within the detection limit of X-ray diffraction pattern for all the ceramic samples. The close examination of the patterns around $2\theta = 33$ – 35° shown in Fig. 1b. The diffraction peaks of the ceramic samples shift toward lower angles with increasing content of Mn, which may be related to the following doped mechanisms.

The slight decrease of diffraction angle with increasing doping concentration implies that Mn^{2+} ions substitute for Ti^{4+} ions and Zn^{2+} ions substitute for Cu^{2+} ions. And cause an increasing cell volume due to the substitution of larger Mn^{2+} ions radius for smaller Ti^{4+} ions and Zn^{2+} ions radius for smaller Cu^{2+} ions. When further increasing

the doping concentration to $y = 0.05$, the slightly decreased diffraction angle suggests that Mn^{2+} ions may substitute for Ti^{4+} ions partly, and the remainder of Mn^{2+} ions may concentrate at the grain boundaries. This doped mechanism is consistent with the corresponding microstructure later (Fig. 2).

Figure 2 presents the SEM micrographs of the ceramic samples sintered at 1060 °C for 8 h. As shown in Fig. 2, the pure CCTO ceramic shows a large-grained microstructure with grain sizes of about 2.1–11.6 μm (Fig. 2a). Substitution of Zn and Mn in CCTO greatly affects the microstructure. The grain size of CCTOM0 and CCTOM3 ceramics is about 1.5–6.4 and 1.2–4.5 μm , respectively, and the grain size uniformity is enhanced. In general, the grain growth in ceramics is primary driven by grain boundary (GB) mobility, which is controlled by the diffusion of ions, atoms, and/or charge species of the grain across the GB. The decrease in grain size of CCTOM3 ceramics may be due to a reduced GB mobility. The improved morphologies could enhance the electrical properties. Compared with CCTOM3 sample, CCTOM5 ceramic exhibit inhomogeneous microstructure, which shows large grains coexist with lots of small ones and with grain size of about 0.8–4.5 μm . It may be due to excess amounts of Mn^{2+} ions concentrate at the grain boundaries and inhibit local grain growth.

The dielectric constant ϵ_r and loss $\tan \delta$ as a function of frequency is shown in Fig. 3. It is worth noting that the substitution of Zn^{2+} and Mn^{2+} ions has not only a great influence on the microstructure of the CCTO ceramics, but also a significant effect on their dielectric properties. Compared with the undoped CCTO samples, CCTOM0, CCTOM3 and CCTOM5 samples exhibit a low ϵ_r . The ϵ_r at 10 kHz is 10,680, 7705, 6620, and 5785 for CCTO, CCTM0, CCTM3, and CCTM5, respectively. The difference in ϵ_r can be attributed to the difference in the grain

Fig. 1 XRD patterns of CCTO, CCTOM0, CCTOM3 and CCTOM5 ceramics

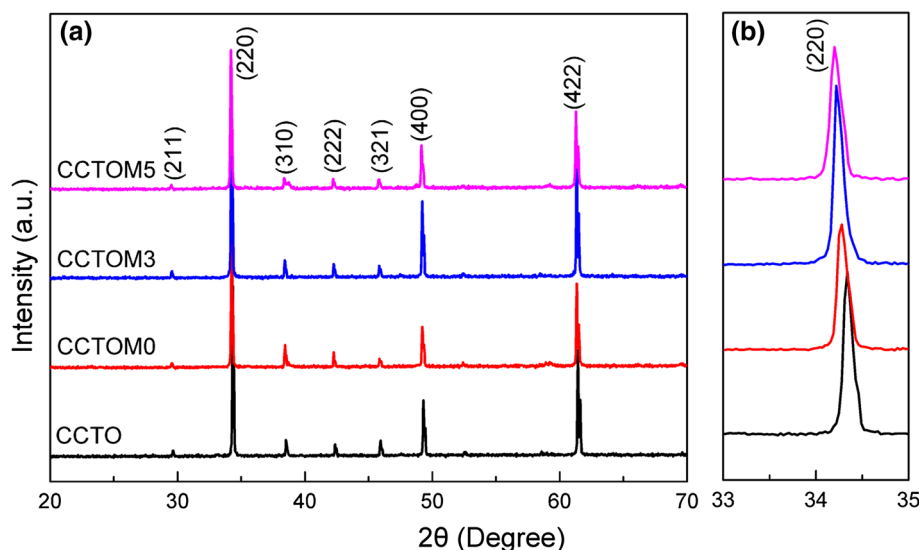


Fig. 2 SEM images of pure CCTO and doped CCTO ceramic. **a** CCTO, **b** CCTOM0, **c** CCTOM3, and **d** CCTOM5

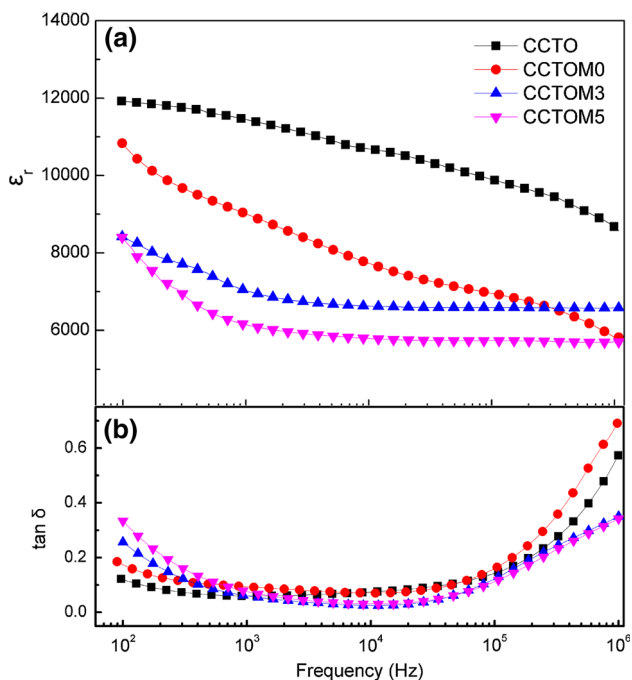
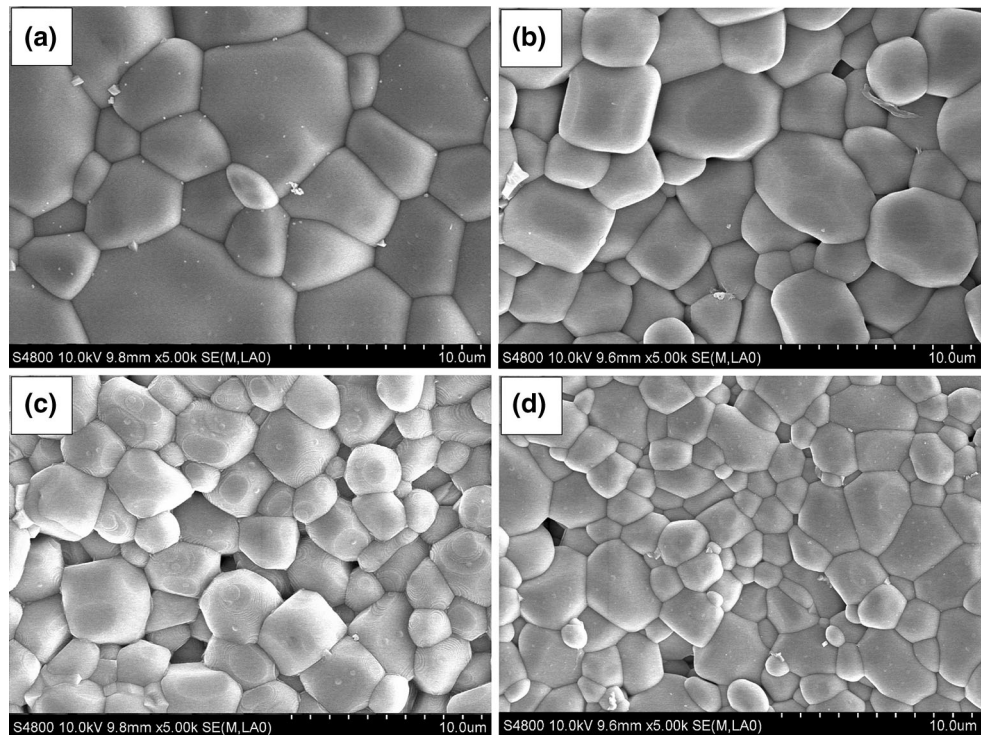


Fig. 3 Dielectric constant (a) and dielectric loss (b) as function of frequency for pure CCTO and doped CCTO ceramics

size distribution. Mn and Zn doped CCTO ceramics have smaller dielectric constant than the pure CCTO ceramic sample. It may be due to the smaller grain size and higher Cu^{2+} vacancy concentration for Mn and Zn doped CCTO ceramic samples. It is well known, smaller grains

associated with lower dielectric constants. Moreover, dielectric constant of CCTO ceramics is influenced by the Cu^{2+} vacancy concentration which can improve potential barrier height and increase nonlinear coefficient, and lead to a low dielectric constant [6]. This result is similar to those observed in literature for Mn doped CCTO ceramics [18]. Although the Zn and Mn co-doping reduces ϵ_r , it can effectively improve the $\tan \delta$ in the medium frequency region and at around room temperature. The $\tan \delta$ at 10 kHz is 0.074, 0.071, 0.026, and 0.03 for CCTO, CCTM0, CCTM3, and CCTM5, respectively. The low $\tan \delta$ in CCTOM3 may be attributed to the high grain boundary resistances R_{gb} (Fig. 5) and low leakage current. It was reported that Zn doped CCTO have low leakage current and low loss [6], and Mn doped CCTO have high R_{gb} [13]. However, this result is still insufficient to explain the origin of dielectric response in CCTO ceramics. Variations of other parameters caused by Zn^{2+} and Mn^{2+} substitution need to be suitably modeled.

The temperature dependence of ϵ_r and $\tan \delta$ of the pure CCTO and doped CCTO ceramic samples are plotted in Fig. 4. It shows that ϵ_r increases with increasing temperatures. It may be due to the ability of the charge carriers to align with the applied field increases at higher temperatures, resulting in increase of ϵ_r [19]. Furthermore, at higher temperature, polarization increases because of the accumulation of charge carrier at the interface between samples and electrode [20].

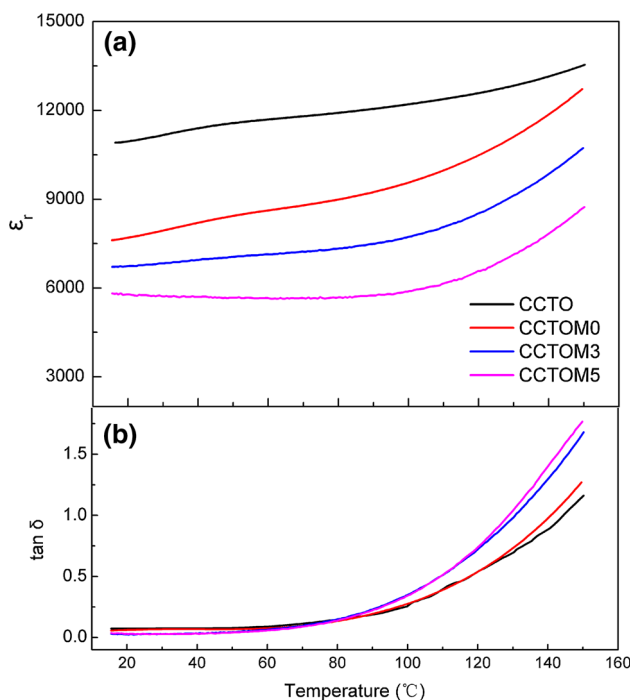


Fig. 4 Temperature dependence of dielectric constant (a) and dielectric loss (b) at 10 kHz for pure CCTO and doped CCTO ceramics

The values of $\tan \delta$ of all ceramic samples increase slightly from room temperature to 80 °C, and thereafter they increase rapidly with increasing temperature to 150 °C. It is due to the increase in conductivity with increase in temperature [21]. The $\tan \delta < 0.035$ in the temperature range of 15–40 °C at 10 kHz for the CCTOM3 ceramics was achieved. Certain Zn and Mn co-doping effectively reduced the $\tan \delta$.

Figure 5 shows the impedance spectroscopy plots of all the CCTO ceramics at room temperature. The inset figure shows the expanded view of the impedance plane plots

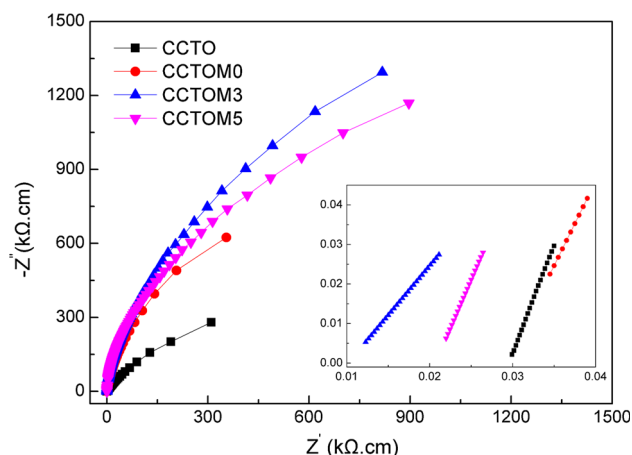


Fig. 5 Impedance complex plane plots for pure CCTO and doped CCTO ceramics. The inset shows an expanded view of the high frequency data close to the origin

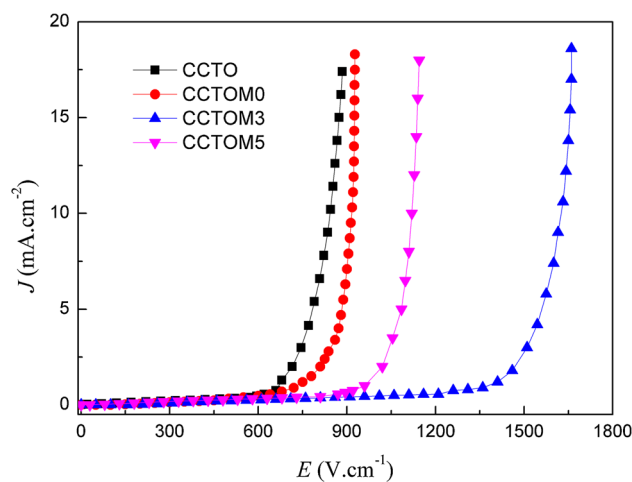


Fig. 6 Nonlinear $J-E$ characteristics at room temperature for all ceramic samples

in the high-frequency region, which is the electrical response of ceramics samples grains. For all samples, only a semi-circular arc was observed with a non-zero intercept on the real axis at a high frequency. It can be seen that the addition of Zn and Mn has a great influence on the resistivity of grain and grain boundary, especially for the grain boundary. The more stability of grain boundary resistance R_{gb} for CCTOM3 sample at the broad range of frequencies is responsible for low loss.

Figure 6 shows the nonlinear electrical characteristics of pure CCTO and doped CCTO ceramic samples. Although all the ceramic samples exhibited nonlinear $J-E$ behavior, different characteristics were observed in Zn^{2+} and Mn^{2+} co-doped CCTO ceramic. The nonlinear coefficient α are 2.5, 3.5, 4.3, and 3.8 for CCTO, CCTOM0, CCTOM3, and CCTOM5, respectively. The breakdown electric field E_b are 576, 672, 1285, and 843 V/cm for CCTO, CCTOM0, CCTOM3, and CCTOM5, respectively. It is seen that the Zn and Mn doping improves the nonlinear property of the ceramic by enhancing α and E_b . It is known that the nonlinear electrical properties of CCTO are attributed to the existence of electrostatic potential barriers at the GBs [22, 23]. The potential barrier height is related to the surface states existing at grain boundaries and the other intrinsic electronic parameters of grains. The increase of E_b in Zn^{2+} and Mn^{2+} doped CCTO ceramics is primarily associated with an increase in the Schottky barrier. Furthermore, the variation in E_b is consistent with R_{gb} values [24].

4 Conclusion

In conclusion, Zn-doped and (Zn+Mn) co-doped $CaCu_3Ti_4O_{12}$ ceramics were successfully prepared by the citrate-nitrate combustion derived powders. The results of

microstructure and dielectric measurement showed that both microstructure and dielectric properties exhibited strong dependence on doping conditions. The doping of Zn and Mn can effectively reduce the dielectric loss in the medium frequency region and enhances the nonlinear J – E properties.

Acknowledgments This work was supported by Science and technology funding projects of Chongqing Municipal Education Commission (KJ1501601).

References

1. M.A. Subramanian, D. Li, N. Duan, B.A. Reisner, A.W. Sleight, *J. Solid State Chem.* **151**, 323 (2000)
2. C.C. Homes, T. Vogt, S.M. Shapiro, S. Wakimoto, A.P. Ramirez, *Science* **293**, 673 (2001)
3. Y. Yang, X. Wang, B. Liu, *J. Mater. Sci. Mater. Electron.* **25**, 146 (2014)
4. Y. Huang, D. Shi, Y. Li, G. Li, Q. Wang, L. Liu, L. Fang, *J. Mater. Sci. Mater. Electron.* **24**, 1994 (2013)
5. X. Ouyang, M. Habib, P. Cao, S. Wei, Z. Huang, W. Zhang, W. Gao, *Ceram. Int.* **41**, 13447 (2015)
6. D. Xu, K. He, R. Yu, X. Sun, Y. Yang, H. Xu, H. Yuan, J. Ma, *Mater. Chem. Phys.* **153**, 229 (2015)
7. Z. Xu, H. Qiang, Z. Chen, Y. Chen, *J. Mater. Sci. Mater. Electron.* **26**, 578 (2015)
8. M.F.A. Rahman, S.D. Hutagalung, Z.A. Ahmad, M.F. Ain, J.J. Mohamed, *J. Mater. Sci. Mater. Electron.* **26**, 3947 (2015)
9. Y. Liu, Q. Chen, X. Zhao, *J. Mater. Sci. Mater. Electron.* **25**, 1547 (2014)
10. Y. Hu, T.S. Ieng, J.S. Liu, T.C. Liu, C.C. Lin, *Adv. Appl. Ceram.* **113**, 98 (2014)
11. F.C. Luo, J.L. He, J. Hu, Y.H. Lin, *J. Am. Ceram. Soc.* **93**, 3043 (2010)
12. P. Thongbai, J. Jompatam, B. Putasaeng, T. Yamwong, S. Maensiri, *Mater. Res. Bull.* **60**, 695 (2014)
13. M. Li, A. Feteira, D.C. Sinclair, A.R. West, *Appl. Phys. Lett.* **88**, 232903 (2006)
14. C.H. Kim, Y.H. Jang, S.J. Seo, C.H. Song, J.Y. Son, Y.S. Yang, J.H. Cho, *Phys. Rev. B* **85**, 245210 (2012)
15. H. Qiang, Z. Xu, *J. Mater. Sci. Mater. Electron.* **27**, 9976 (2016)
16. P. Thongbai, S. Pinitsoontorn, V. Amornkitbamrung, T. Yamwong, S. Maensiri, P. Chindaprasirt, *Int. J. Appl. Ceram. Technol.* **10**, E77 (2013)
17. Z. Xu, H. Qiang, *J. Sol–Gel. Sci. Technol.* **77**, 650 (2016)
18. F. Amaral, E. Clemente, M.A. Valente, L.C. Costa, F.M. Costa, *Ceram. Int.* **40**, 16503 (2014)
19. O. Parkash, D. Kumar, A. Goyal, A. Agrawal, A. Mukherjee, S. Singh, P. Singh, *J. Phys. D Appl. Phys.* **41**, 035401 (2008)
20. I. Norezan, A.K. Yahya, M.K. Talari, *J. Mater. Sci. Technol.* **28**, 1137 (2012)
21. B.S. Prakash, K.B.R. Varma, *J. Phys. Chem. Solids* **68**, 490 (2007)
22. T. Adams, D. Sinclair, A. West, *Phys. Rev. B: Condens. Matter* **73**, 094124 (2006)
23. A.A. Felix, M.O. Orlandi, J.A. Varela, *Solid State Commun.* **151**, 1377 (2011)
24. J. Boonlakhorn, P. Kidkhunthod, P. Thongbai, *J. Eur. Ceram. Soc.* **35**, 3521 (2015)